PAPER

NJC
www.rsc.org/njc

Theoretical study of tri-s-triazine and some of its derivatives

Wenxu Zheng,[a] Ning-Bew Wong,*[b] Ge Zhou,[a] Xiaoqin Liang,[a] Jinshan Li[c] and Anmin Tian*[a]

[a] *Faculty of Chemistry, Sichuan University, Chengdu 610064, People's Republic of China. E-mail: suqcp@mail.sc.cninfo.net*
[b] *Department of Biology and Chemistry, City University of Hong Kong, Kowloon, Hong Kong*
[c] *China Academy of Engineering Physics, Mianyang 621900, People's Republic of China*

Received* (in Montpellier, France) *27th August 2003, Accepted 14th October 2003
First published as an Advance Article on the web 15th January 2004

Density functional theory has been used to study the geometries, electronic structures, harmonic vibrational frequencies, and high energy density material properties of tri-s-triazine and ten derivatives (2-R-5,8-dihydrogen-tri-s-triazine with R = NH_2, OH, N_3, NO_2, F, Cl, Br, –C≡N, –CH=CH_2 and –C≡CH) at the B3LYP/aug-cc-pVDZ level of theory. The results show that the tri-s-triazine ring maintains a planar and rigid structure in all the compounds and that there exists considerable conjugation over the parent ring, which is advantageous for the stability of these compounds. Substituent effects on the geometry, electronic structure, conjugation and HOMO/LUMO of the parent ring are discussed in detail. Vibrational frequency studies indicate that the parent ring has a characteristic frequency and that all the studied substituents shift it to lower wave numbers. Moreover, our study shows that some of the discussed compounds may be potential candidates for high energy density materials (HEDMs).

1. Introduction

s-Triazine based chemicals have been applied variously in the manufacture of polymers, dyes, explosives, pesticides and commodity chemicals.[1] As a consequence, theoretical and experimental studies on these chemicals have been widely carried out,[2] with the result that the s-triazine ring is known as an important conjugated heterocycle whose electronic properties are expected to show subtle differences from those of benzene due to the alternate replacement of CH groups by nitrogen atoms. Some researchers have indicated that the formation of molecular complexes (*e.g.*,, di-, tri-, oligo- and polymers) is a conceivable way to increase density and stability and to improve the material properties of these chemicals.[3] Our interest is focused on tri-s-triazine based chemicals whose C_6N_7 nucleus consists of three fused s-triazine rings. In fact, investigations on these compounds date back to the 1830s.[4,5] At that time, a group of related nitrogen compounds, such as melem, hydromelonic acid, cyameluric chloride, cyameluric acid, *etc.*, were known for their high heat stability, low solubility and low chemical reactivity. However, because of their insolubility and chemical inertness, these compounds remained structural puzzles for more than a century. In 1937, Pauling and Sturdivant[6] first suggested a formulation for their common nucleus, a coplanar arrangement of three fused s-triazine rings. Pauling apparently maintained an interest in tri-s-triazine, for reasons unknown, as the molecular formula of 2-azido-5,8-dihydroxy-tri-s-triazine was preserved on his office chalkboard at the time of his death in 1994.[7] However, in the past decades, only tri-s-triazine, $C_6N_7H_3$, has been studied in detail.[8–11] Its structural and spectroscopic properties, including an X-ray crystal structure analysis, have been discussed. UV photoelectron spectra were taken and *ab initio* calculations performed in order to explain its low basicity and the high stability.[8–11] In 2002, Kroke *et al.* reported the synthesis and detailed structural characterization of a functionalized tri-s-triazine derivative, 2,5,8- trichloro-tri-s-triazine.[12] To our knowledge, other compounds containing the tri-s-triazine unit have been only briefly mentioned in communications or patents and were not characterized at all.[13]

The aim of our work is to systemically study the geometric and electronic structures and properties of tri-s-triazine-based chemicals using a theoretical approach. We have investigated the features of tri-s-triazine and some of its trisubstituted derivatives. The substituents selected in our study are NH_2, OH, N_3, NO_2, –C≡N, F, Cl, Br, –CH=CH_2 and –C≡CH. In our previous work,[14] we have studied one of the substitution patterns, with all three substituents in each derivative being the same. In this paper, we will discuss another substitution pattern: only one of the hydrogens of tri-s-triazine is substituted by the substituents mentioned previously.

2. Methods

Density functional theory (DFT)[15] has been applied to optimize all the structures and to predict harmonic vibrational frequencies. Becke's three-parameter nonlocal exchange functional along with the Lee–Yang–Parr nonlocal correlation functional (B3LYP) was employed.[16,17] Dunning's aug-cc-pVDZ (5d) basis set has been used throughout[18] and the SCF convergence criterion was set to 10^{-8}. The natural bond orbital (NBO)[19–22] analysis has been carried out at the B3LYP/aug-cc-pVDZ level based on the optimized geometries. All these calculations were carried out using the Gaussian 98 program.[23]

The topological properties of the electronic charge density have been characterized using the atoms in molecules methodology (AIM)[24] with the AIM 2000 program package.[25]

Some of molecules discussed in this paper may be novel candidates for high energy density materials (HEDMs). To evaluate their HEDM performance, we have calculated their heats of formation and the relative specific impulse values introduced by Politzer *et al.*[26] The specific impulse (I_S), widely used as a means of characterizing and evaluating propellants, is often expressed in terms of the absolute temperature in the combustion chamber, T_C, and the number of moles of gaseous

DOI: 10.1039/b310375g

products produced per unit weight of propellants N ($N = n/M$, where n is the number of moles of gaseous products produced by one mole of propellants, and M is the molecular weight of propellants) by the simplified relationship given as eqn. (1):[27]

$$I_S \sim T_C^{1/2}\, N^{1/2} \quad (1)$$

This proportionality can be rationalized by kinetic theory. In order to apply eqn. (1), it is necessary to establish the identities and amounts of the various products and to determine the combustion temperature. Depending upon the composition of the propellants, the major components of the gaseous products may include CO, CO_2, N_2, H_2O and/or HF, with lesser quantities of other molecules and radicals such as H_2, NO, H, C, O, CHO and N_2O.[26]

A simple approach to obtaining a rough approximation of the combustion temperature involves assuming that the heat of combustion of the propellants is used entirely to heat the product gases to the combustion temperature, so that

$$-\Delta H_{comb} = C_{p,gases}(T_C - T_0) \quad (2)$$

and

$$T_C = T_0 - \frac{\Delta H_{comb}}{C_{P,gases}} \quad (3)$$

ΔH_{comb} is the enthalpy of combustion, $C_{p,gases}$ represents the total heat capacity of the gaseous products, and T_0 and T_C are the initial and the combustion temperatures. In eqns. (2) and (3), it is assumed that ΔH_{comb} is constant over the temperature range between $T_0$and T_C, and that the pressure in the combustion chamber remains constant due to a steady-state situation; the rates of formation and discharge of product gases are taken to be equal.ΔH_{comb} can be calculated from the molar heats of formation of the propellants and the gaseous products [eqn. 4]:

$$\Delta H_{comb} = \sum_{i}^{products} N_i \Delta H_{f,i} - N_{HEDM}\Delta H_{f,HEDM} \quad (4)$$

The latter are known, while the former can be determined in a number of ways; for example, a reasonable estimate can often be obtained from standard bond enthalpies plus any strain contributions. Politzer *et al.*[26] have pointed out that the relative specific impulse is not highly sensitive to the method used for obtaining the heats of formation. In our work, we compute gas phase heats of formation with the semi-empirical AM1 method.

3. Results and discussion

3.1. Properties of tri-s-triazine

We have investigated the geometric and electronic structure of the tri-s-triazine composed of three s-triazines at the B3LYP/aug-cc-pvDZ level. s-Triazine, a high symmetry molecule with an aromatic hetero-ring, and the all-carbon equivalent of tri-s-triazine, 9b*H*-phenalene anion, are used as the reference molecules.

Lancaster and Stoicheff had determined the geometrical structure of s-triazine in the gas phase by a Raman study.[28] Compared with their experimental results, our optimized structural parameters show good agreement (see Fig. 1). So the computational methods we use in this paper are reliable. As shown in Fig. 1, tri-s-triazine has a rigid planar geometry with D_{3h} symmetry. The N1–C2, C2–N3, N4–C5, C5–N6, N7–C8 and C8–N9 bond lengths are 1.334 Å, the N1–C9a, N3–C3a, C3a–N4, N6–C6a, C6a–N7 and N9–C9a bond lengths are 1.337 Å, and the C3a–N9b, C6a–N9b and C9a–N9b bond lengths are 1.407 Å. Corresponding experimental data[9] are listed in the Fig. 1. We find that the periphery of this tricyclic system has a uniform bond length distribution, with C–N bond lengths intermediate to the normal C–N single (1.470 Å)[29] and C=N double (1.280 Å) bond lengths.[29] A delocalized system seems to exist over tri-s-triazine. Judging from the natural bond orbital (NBO) analysis, the Wiberg bond indexes (WBIs)[20] (see Table 1) of N1–C2, C2–N3, N4–C5, C5–N6, N7–C8 and C8–N9 are 1.40, while the WBIs of N1–C9a, N3–C3a, C3a–N4, N6–C6a, C6a–N7 and N9–C9a are 1.34. These WBIs are similar to the WBIs of C–N bonds in s-triazine (1.41). The fact that all the WBIs are between the standard values of the single bond (1.0) and the double bond (2.0) indicates considerable conjugation over the ring. In addition, the stabilization interaction energies $E(2)$ are calculated by means of second-order perturbation theory. In the NBO analysis, $E(2)$ is used to describe the delocalization trend of electrons from the donor bond to the acceptor bond. Selected values of $E(2)$ for tri-s-triazine at the B3LYP/aug-cc-pVDZ level are summarized in Table 2 and Fig. 2, where BD and BD* represent bonding and antibonding natural bond orbitals and LP represents lone pairs. As shown in Table 2 and Fig. 2, there are strong donor-acceptor interactions in this system. Interaction energies $E(2)$ between π bonding orbitals and π* antibonding orbitals on the periphery of the system are 43.37 kcal mol^{-1}, and $E(2)$ values between a lone pair of the central nitrogen atom and peripheral π* antibonding orbitals are about 49.10 kcal mol^{-1}. These $E(2)$ are similar to the $E(2)$ between π bonding orbitals and π* antibonding orbitals in s-triazine (38.01 kcal mol^{-1}). Moreover, molecular orbital analysis shows the presence of a delocalized occupied π orbital in tri-s-triazine (A). This orbital is composed purely of the $2p_z$ orbitals of all the carbon and nitrogen atoms; its stereograph is drawn in Fig. 3.

As discussed above, we see that the tri-s-triazine (**A**) molecule contains a large conjugation system, which suggests that this structure is stable. We have analyzed its topological properties of electron density using Bader's theory of atoms in molecules (AIM).[24] The AIM atomic charges listed in Table 3 indicate that the formation of tri-s-triazine results in electron redistribution among the nitrogen and carbon atoms, compared with that in s-triazine. The net charge on each of the carbon atoms is +1.11, while it is −1.08 for all the nitrogen atoms in s-triazine. After formation of tri-s-triazine, the positive charge on each of the carbon atoms is increased, while all the negative charges on the nitrogen atoms decrease except for N_{9b}, which shows no change. A more sensitive probe of the electronic structure of a molecule is provided by the Laplacian of the charge density, $\nabla^2_\rho(r)$, which determines the regions of space wherein the electronic charge of a molecule is locally concentrated and depleted.[30] This function has been shown to demonstrate the existence of local concentrations of electronic charge in both bonded and non-bonded regions of an atom in a molecule,[30,31] without recourse to any orbital model or arbitrary reference state. Interactions resulting from the sharing of charge density between atoms, as in covalent and polar bonds, are characterized by $\nabla^2_\rho(r) < 0$. The contours of the Laplacian of the charge density of s-triazine and tri-s-triazine are drawn in Fig. 4, which clearly indicate that $\nabla^2_\rho(r)$ in tri-s-triazine remains very similar to that in s-triazine; the electron cloud around each nitrogen atom shows a much greater concentration of charge and a small polarization of the covalent CN bond with the lone pairs on the nitrogen atoms is clearly visible, while the nitrogen lone pairs in tri-s-triazine are less diffuse than their counterparts in s-triazine. Here it should be emphasized that non-bonded charge concentrations are thinner in radial extent than are the bonded ones.

Vibrational analysis shows that tri-s-triazine has a characteristic frequency at 870 cm^{-1}. Its vibrational mode is C,N out-of-plane rocking, with an infrared intensity of 35 km mol^{-1}. This vibrational mode has not been found in s-triazine,

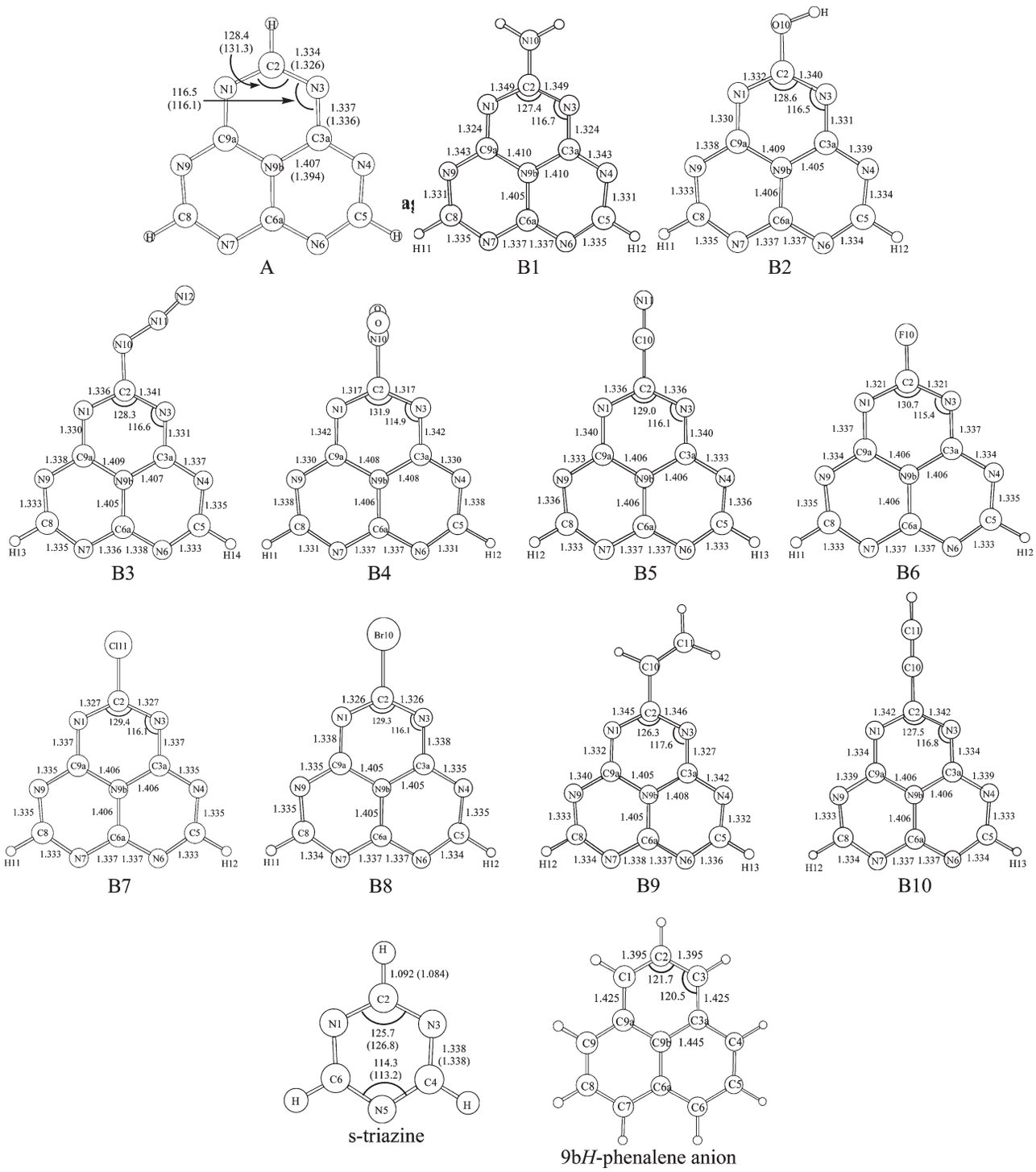

Fig. 1 Optimized molecular structures for s-triazine, 9b*H*-phenalene anion, tri-s-triazine (**A**) and its ten derivatives (**B1**–**B10**) along with their bond lengths (in Å) and angles (in °). Experimental data for s-triazine and tri-s-triazine are listed in parentheses.

thus it can be used to distinguish s-triazine and tri-s-triazine. This difference may be useful for experimental synthesis and recognition of tri-s-triazine.

3.2. Properties of some derivatives of tri-s-triazine

Many organic chemicals show various profound features by replacing their substituents. In this section, we will discuss the geometric and electronic properties of some derivatives of tri-s-triazine, 2-R-5, 8-dihydrogen-tri-s-triazine. The substituents (R) that we selected include electron-donating and electron withdrawing groups and halogens: $–NO_2$, $–NH_2$, $–N_3$, –OH, –C≡N, –F, –Cl, –Br, $–CH–CH_2$ and –C≡CH.

3.2.1. Geometry. We have first optimized the geometries of these derivatives at the B3LYP/aug-cc-pvDZ level. The optimized structures along with their geometrical parameters are illustrated in Fig. 1. Vibrational analysis shows there are no imaginary frequencies for all the structures at this theoretical level, which suggests that all the structures we obtained are local minima on the potential energy surface. It is clear that almost all the derivatives have C_{2v} symmetry, while **B2**, **B3** and **B9** have C_s symmetry. The ring retains its rigid plane in

Table 1 The Wiberg bond indexes of the bonds in the ring for tri-s-triazine (**A**) and its ten derivatives (**B1**–**B10**)

	A	B1	B2	B3	B4	B5	B6	B7	B8	B9	B10
N1–C2	1.40	1.28	1.33	1.33	1.42	1.37	1.38	1.38	1.39	1.34	1.34
N2–C3	1.40	1.27	1.31	1.32	1.42	1.37	1.38	1.38	1.39	1.32	1.34
N4–C5	1.40	1.42	1.40	1.40	1.38	1.38	1.39	1.39	1.39	1.41	1.40
C5–N6	1.40	1.39	1.40	1.40	1.41	1.41	1.41	1.40	1.40	1.39	1.39
N7–C8	1.40	1.39	1.39	1.39	1.41	1.41	1.41	1.40	1.40	1.40	1.39
C8–N9	1.40	1.42	1.41	1.41	1.38	1.38	1.39	1.39	1.39	1.40	1.40
N1–C9a	1.34	1.40	1.37	1.36	1.30	1.32	1.33	1.33	1.33	1.35	1.35
N3–C3a	1.34	1.40	1.36	1.35	1.30	1.32	1.33	1.33	1.33	1.37	1.35
N9–C9a	1.34	1.32	1.33	1.34	1.37	1.36	1.35	1.35	1.35	1.33	1.34
N4–C3a	1.34	1.32	1.34	1.34	1.37	1.36	1.35	1.35	1.35	1.32	1.34
N6–C6a	1.34	1.34	1.34	1.34	1.34	1.34	1.34	1.34	1.34	1.34	1.34
N7–C6a	1.34	1.34	1.35	1.35	1.34	1.34	1.34	1.34	1.34	1.34	1.34
C3a–N9b	1.04	1.02	1.04	1.04	1.04	1.04	1.04	1.04	1.04	1.03	1.04
C6a–N9b	1.04	1.04	1.04	1.04	1.05	1.04	1.04	1.04	1.04	1.04	1.04
C9a–N9b	1.04	1.02	1.03	1.03	1.04	1.04	1.04	1.04	1.04	1.04	1.04

all the derivatives, and all the hydrogens and substituents are in this plane except for the NO_2 group.

Compared to the tri-s-triazine ring, the lengths of C–N bonds adjacent to the substituents are changed considerably in the derivatives. In the vicinity of substituents, the C–N bond lengths are 1.349, 1.340, 1.341, 1.317, 1.336, 1.321, 1.327, 1.326, 1.346 and 1.342 Å in **B1** to **B10**, respectively. Compared with the corresponding bond length of 1.334 Å in the parent molecule **A**, it is clear that when an electron-donating group, such as $–NH_2$, $–N_3$ or –OH, is attached to the parent ring, the adjacent C–N bond lengths increase. The converse is true when an electron-withdrawing group or a halogen, such as $–NO_2$, –F, –Cl or –Br, is attached to the parent ring. When a substituent containing a π bond, such as –C≡N, $–CH=CH_2$ and –C≡CH, is attached to the parent ring, the adjacent C–N bond lengths increase.

Compared with these changes in bond lengths, the bond angles adjacent to the substituents only change slightly. The $N_1–C_2–N_3$ and $C_2–N_3–C_{3a}$ bond angles are 128.4° and 116.5° in tri-s-triazine **A**, but in the derivatives, these two bond angles only change to 127.4° and 116.7°, 128.6° and 116.5°, 128.3° and 116.6° , 131.9° and 114.9°, 129.0° and 116.1° , 130.7° and 115.4°, 129.4° and 116.1° , 129.3° and 116.1°, 126.3° and 117.6°, and 127.5° and 116.8° for **B1** to **B10**, respectively. We find that these two bond angles change considerably only in **B4**.

Table 2 Selected stabilization interaction energies $E(2)$ for tri-s-triazine (**A**) and its ten derivatives (**B1**–**B10**)

	Donor NBO	Acceptor NBO	$E(2)$/kcal mol^{-1}
	BD N1–C2	BD* N9–C9a	43.37
	BD N9–C9a	BD* N7–C8	43.37
	BD N7–C8	BD* N6–C6a	43.37
	BD N6–C6a	BD* N4–C5	43.37
	BD N4–C5	BD* N3–C3a	43.37
	BD N3–C3a	BD* N1–C2	43.37
	LP(1) N9b	BD* N3–C3a	49.10
	LP(1) N9b	BD* N6–C6a	49.10
A			
LP(1) N9b	BD* N9–C9a	49.10	
B1	LP(1) N10	LP* C2	130.13
B2	LP(2) O10	BD* C2–N3	46.13
B3	BD N1–C9a	BD* C2–N10	46.85
B5	BD C10–N11	BD* N1–C2	11.51
B6	LP(3) F10	BD* N1–C2	29.18
B7	LP(3) Cl10	BD* N1–C2	20.30
B8	LP(3) Br10	BD* N1–C2	16.04
B9	BD C10–C11	BD* N1–C2	19.93
B10	BD C10–C11	BD* N1–C2	17.68

3.2.2. Electronic structure. These geometric variations in the derivatives are consistent with the topological properties of electron density at the bond critical points. The Laplacian of the electron density, $\nabla^2_\rho(r)$, at the bond critical points of the C–N bond adjacent to the substituents is, respectively, −1.144, −1.196, −1.176, −1.300, −1.224, −1.316, −1.260 , −1.264, −1.176 and −1.188 for **B1** to **B10**, respectively. Compared with the corresponding $\nabla^2_\rho(r)$of −1.232 for the parent molecule **A**, it is worth stressing that the introduction of electron-withdrawing groups and halogens makes $\nabla^2_\rho(r)$ more negative, which means that the corresponding C–N bond is

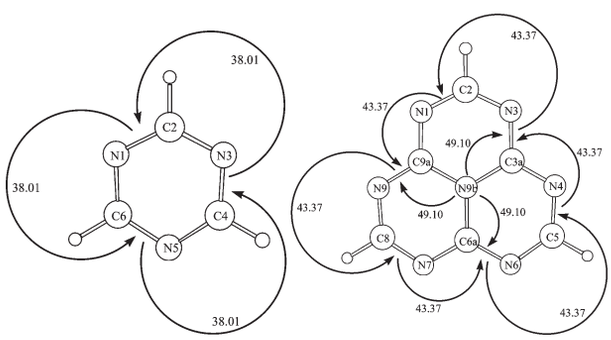

Fig. 2 The stabilization interactions [$E(2)$ in kcal mol^{-1}] between π bonding orbitals and π* antibonding orbitals and between lone pair and π* antibonding orbitals in s-triazine and tri-s-triazine.

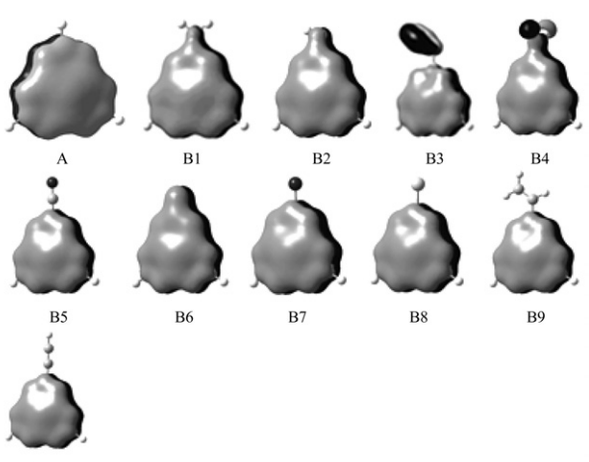

Fig. 3 The delocalized occupied π orbitals in tri-s-triazine (**A**) and its ten derivatives (**B1**–**B10**).

Table 3 The AIM atomic charges for s-triazine and tri-s-triazine

s-Triazine		Tri-s-triazine	
Atom	Charge[a]	Atom	Charge[a]
N1	−1.08	N1	−0.97
C2	1.11	C2	1.18
N3	−1.08	N3	−0.99
C4	1.11	C3a	1.43
N5	−1.08	N4	−0.99
C6	1.11	C5	1.18
		N6	−0.99
		C6a	1.43
		N7	−0.98
		C8	1.18
		N9	−0.97
		C9a	1.43
		N9b	−1.08

[a] The integration radius is 0.5 a.u. for all the atoms.

strengthened. Conversely, $\nabla^2_\rho(r)$ is less negative when an electron-donating group or a substituent containing a π bond is attached, which means that the corresponding C–N bond is weakened. However, the variation of $\nabla^2_\rho(r)$ at the bond critical points of the N9b–C bonds is very small as they are all about −0.84 in tri-s-triazine **A** and its derivatives **B**, which indicates that the substitutent effect on the N9b–C bond is slight.

The electron distribution of a molecule can also be described by the molecular electrostatic potential (MEP).[32–34] The electrostatic potential at a spatial point r around a molecule is (in atomic units):[35]

$$V(r) = \sum_A \frac{Z_A}{|R_A - r|} - \int \frac{\rho(r')}{|r - r'|} dr' \qquad (5)$$

where Z_A is the charge on nucleus A located at R_A. The first term on the right-hand side of eqn. (5) represents the effect of the nuclei and the second is that of the electron density. $V(r)$ is then the net electrostatic effect resulting from the total molecular charge distribution (nuclei plus electrons). The sign of $V(r)$ indicates the regions where either nuclei or electrons dominate, so that an approaching electrophile will be drawn to points where $V(r) < 0$, and particularly the local minima. The MEP is an important analytical tool in the study of molecular reactivity, and it is particularly useful when visualized on surfaces or in regions of space, since it provides information about local polarity. Typically, after having chosen the region to be visualized, a color-coding convention is chosen to depict the MEP.[36] In this paper, the most negative potential is assigned to be black, the most positive potential is assigned to be white, and the color spectrum is mapped to all other values by linear interpolation. Fig. 5 summarizes the shape and position of the MEP observed. The electrostatic behavior of these molecules as given by MEP shows a clear and marked separation between the negative spatial domains and the positive domain that covers the entire space surrounding the ring. When an electron-donating group (–NH_2, –N_3, –OH) is attached to the parent ring, the negative spatial domains are extended mildly. The same result can be obtained by the attachment of a substituent containing a π bond (–CH=CH_2, –C≡CH) to the parent ring. However, if the substituent is a halogen, the negative spatial domains shrink. –NO_2 and –C≡N are special. When these two groups are attached to the ring, the negative spatial domains split and shrink, and the new negative spatial domains emerge near the nitryl oxygen and cyanophoric nitrogen.

The net charge distributions in the studied compounds were analyzed by means of natural bond orbital (NBO) analysis. In Table 4, we list selected natural atomic charges. The results indicate that all the substituents increase the magnitude of the positive charge on the connecting carbon C_2. The charges of other atoms in the parent ring show almost no change in all the derivatives.

To investigate the interactions between the substituents and the parent ring, the second-order perturbation stabilization energies $E(2)$ were calculated and are summarized in Table 2. In NBO analysis, if the stabilization interaction energy $E(2)$ between a donor bonding orbital and an acceptor antibonding orbital is large, there is a strong interaction between the two bonds. In Table 2, only the stabilization energies between donor π orbital and acceptor π* orbital or donor lone pair orbital and acceptor π* orbital are listed. $E(2)$ values smaller than 10 kcal mol^{-1} are not included in Table 2, as these interactions may be deemed as weak. According to the data, there are strong donor-acceptor interactions between the lone pair orbitals on nitrogen, oxygen and halogen atoms in the –NH_2, –OH, –F, –Cl, –Br groups and the π* orbitals in the ring. Donor-acceptor interactions also exist between the π orbitals of the –N_3, –C≡N, –CH=CH_2, –C≡CH groups and the π* orbitals in the ring. Only for **B4** are there no strong interactions between –NO_2 and the ring, due to two reasons. First, there is no lone pair on the N(NO_2) atom to provide a lone pair orbital as the donor. Second, the N–O π orbital of the –NO_2group is composed of the $2p_x$ orbitals of the nitrogen and oxygen atoms, while the N–C π orbital of the ring is composed of the $2p_z$ orbitals of the nitrogen and carbon

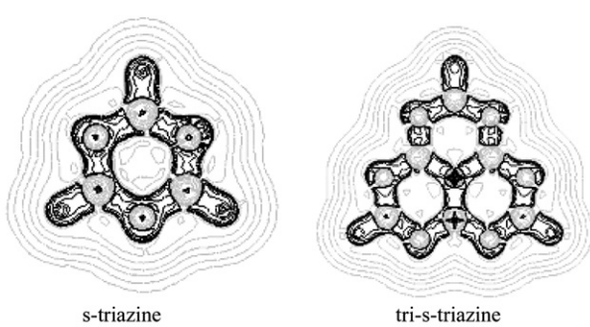

Fig. 4 The contour map of $\nabla^2_\rho(r)$ in the molecular plane for s-triazine and tri-s-triazine (**A**). Positive values of $\nabla^2_\rho(r)$ are denoted by gray contours, negative values by black contours.

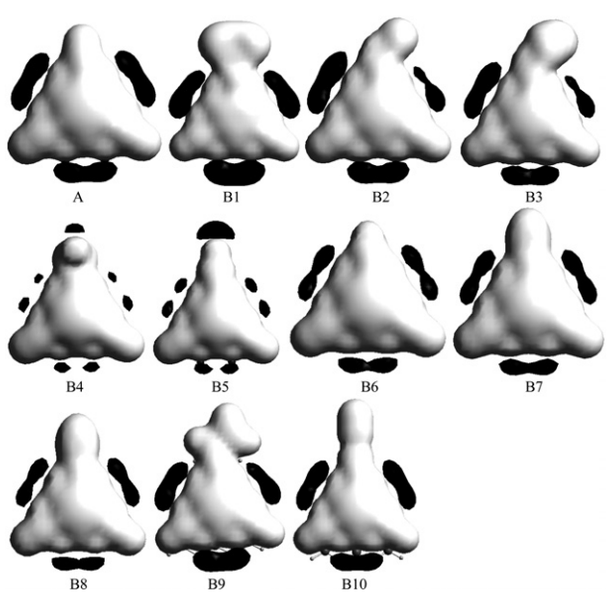

Fig. 5 The MEP surfaces for tri-s-triazine (**A**) and its ten derivatives (**B1**–**B10**).

Table 4 Selected natural atomic charges for tri-s-triazine (A) and its ten derivatives (B_1–B_{10})

	A	B1	B2	B3	B4	B5	B6	B7	B8	B9	B10
N1	−0.55	−0.59	−0.57	−0.54	−0.53	−0.52	−0.57	−0.55	−0.55	−0.55	−0.53
C2	0.36	0.66	0.81	0.64	0.63	0.40	0.90	0.46	0.39	0.48	0.44
N3	−0.55	−0.59	−0.61	−0.59	−0.53	−0.52	−0.57	−0.55	−0.55	−0.56	−0.53
C3a	0.68	0.68	0.68	0.69	0.69	0.69	0.68	0.68	0.69	0.69	0.69
N4	−0.55	−0.56	−0.56	−0.55	−0.53	−0.54	−0.55	−0.54	−0.54	−0.56	−0.55
C5	0.36	0.35	0.36	0.36	0.37	0.36	0.36	0.36	0.36	0.36	0.36
N6	−0.55	−0.56	−0.55	−0.55	−0.54	−0.54	−0.54	−0.54	−0.55	−0.56	−0.55
C6a	0.68	0.68	0.68	0.68	0.68	0.69	0.68	0.68	0.68	0.69	0.69
N7	−0.55	−0.56	−0.55	−0.55	−0.54	−0.54	−0.54	−0.54	−0.55	−0.56	−0.55
C8	0.36	0.35	0.36	0.36	0.37	0.36	0.36	0.36	0.36	0.36	0.36
N9	−0.55	−0.56	−0.55	−0.55	−0.53	−0.54	−0.55	−0.54	−0.54	−0.56	−0.55
C9a	0.68	0.68	0.68	0.68	0.69	0.69	0.68	0.68	0.69	0.69	0.69
N9b	−0.47	−0.48	−0.48	−0.47	−0.46	−0.47	−0.47	−0.47	−0.46	−0.48	−0.47

atoms; the orientations of these two π orbitals are perpendicular, thus preventing the interaction between these two orbitals. As a result of the interaction between substituents and the ring, the natural bond orbital energies of the N–C bond adjacent to the substituents decrease from −0.8816 a.u. for **A** to −0.8900, −0.8906, −0.9364, −0.9106, −0.9141, −0.9192 and −0.9211 a.u. for **B2** to **B8**, respectively, but increase to −0.8631 a.u. for **B1**, −0.8689 a.u. for **B9** and −0.8794 a.u. for **B10**.

3.2.3. Conjugation of the parent ring. From Fig. 1, it can be seen that the bond lengths of the periphery of the ring for all the derivatives range from 1.317 to 1.349 Å, lying between the normal C–N single bond length (1.470 Å)[29] and C=N double bond length (1.280 Å).[29] Judging from these bond lengths, the delocalized system over the ring is also present in the derivatives. Moreover, the Wiberg bond indexes (WBIs) of all the peripheral bonds of the ring are in the range of 1.27–1.41, between the standard values of the single bond (1.0) and the double bond (2.0), indicating considerable conjugation over the ring. In addition, the NBO results show that there exist strong donor-acceptor interactions between π bonding orbitals and π* antibonding orbitals on the periphery of the ring [$E(2)$ is about 40 kcal mol^{-1}] and between the lone pair of the central nitrogen atom and peripheral π* antibonding orbitals [$E(2)$ is about 45 kcal mol^{-1}]. Through molecular orbital analysis, we can find a delocalized occupied π orbital that is composed purely of the $2p_z$ orbitals of all the carbon and nitrogen atoms of the ring in all derivatives. Here we must emphasize that the central nitrogen atom N9b participates in the conjugation, which contributes to the stability of the ring.

3.2.4. HOMO and LUMO. The analysis of the molecular orbitals can provide much useful information about a molecule, such as the site of electron attachment and detachment as well as chemical reactivity.[37] Moreover, HOMO-LUMO gaps are in close agreement with λ_{max} values from UV spectroscopy.[38] According to Koopman's theorem,[39] it is possible to obtain ionization potentials (IP) and electron affinities (EA) from the corresponding HOMO and LUMO eigenvalues in a Hartree-Fock calculation.

The shape and location of the frontier orbitals, that is the HOMO and LUMO, of all the studied molecules is illustrated in Fig. 6. It is observed that all the substituents interact mainly with the LUMO orbital, whereas their interactions with the HOMO are minor. The HOMO of each molecule is localized on the peripheral nitrogen atoms of the ring and has π* antibonding character. It is composed of the $2p_z$ orbitals of these nitrogen atoms. The LUMO is made up of the $2p_z$ orbitals of all the heavy atoms in the molecule.

The calculated results for the HOMO and LUMO energies are listed in Table 5. It shows a comparison of the energetics of different substituted molecules. It is clear from this data that when a $–NH_2$, $–CH=CH_2$ or $–C\equiv CH$ group is attached to the ring, the HOMO energy level increases, whereas the attachment of other groups such as –OH, $–N_3$, $–NO_2$, $–C\equiv N$, –F, –Cl or –Br will decrease the HOMO energy level. As for the LUMO energy level, when a $–NH_2$, –OH, $–N_3$ or $–CH=CH_2$ group is attached to the ring, it will increase and the converse is true when other groups like $–NO_2$, –F, –Cl, –Br, $–C\equiv CH$ or $–C\equiv N$ are attached to the ring.

However, the effects of all halogens, electron-withdrawing and electron-donating groups are found to be similar with respect to the HLG (HOMO-LUMO gap);that is in all cases the derivatives increase the HLG as compared to the parent molecule, reflecting a shift towards higher frequencies in their electronic absorption spectra. But when a group containing a π bond, such as $–CH=CH_2$, $–C\equiv CH$ or $–C\equiv N$, is substituted on the parent ring, the HLG is reduced, reflecting a shift towards lower frequencies in their electronic absorption spectra.

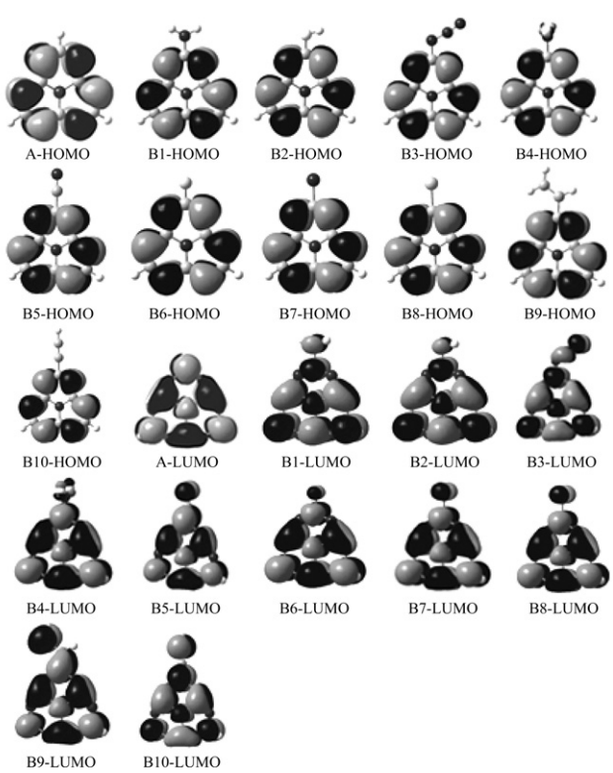

Fig. 6 The HOMO and LUMO molecular orbitals for tri-s-triazine (**A**) and its ten derivatives (**B1**–**B10**).

Table 5 The HOMO and LUMO energies and the energy gap for tri-s-triazine (**A**) and its ten derivatives (**B1**–**B10**)

Molecule	E_{HOMO}/eV	E_{LUMO}/eV	$\Delta E_{LUMO-HOMO}$/eV
A	−7.32	−3.40	3.92
B1	−6.99	−2.78	4.21
B2	−7.34	−3.16	4.18
B3	−7.37	−3.38	3.99
B4	−7.89	−3.92	3.97
B5	−7.78	−4.08	3.70
B6	−7.60	−3.51	4.09
B7	−7.54	−3.54	4.00
B8	−7.52	−3.54	3.98
B9	−7.13	−3.35	3.78
B10	−7.30	−3.55	3.75

3.2.5. Vibrational frequencies. In order to facilitate future experimental verification of tri-s-triazine and its derivatives, the harmonic vibrational frequencies of these compounds are computed at the B3LYP/aug-cc-pVDZ level. Selected harmonic vibrational frequencies and infrared (IR) intensities of tri-s-triazine and its ten derivatives are presented in Table 6. To check the accuracy of our calculated values and to demonstrated the trends in vibrational modes, we also provide in Table 6 the vibrational frequencies and corresponding infrared intensities of 2,4,6-triamino-s-triazine, 2,4,6-trifluoro-s-triazine and 2,4,6-trihydroxyl-s-triazine, computed at the same level of theory, along with their experimental values[40] as available in the literature. According to the data, we find the characteristic frequency of the parent ring is around 850–870 cm^{-1}, corresponding to the C,N out-of-plane rocking. This characteristic frequency is very close to that of s-triazine ring (about 820 cm^{-1}) and all the substituents shift it to higher wave numbers. The infrared intensity of this characteristic frequency ranges from 33 to 42 km mol^{-1} in the derivatives. In comparison, the infrared intensity of the substituent is strong. The intensities of the amino N–H symmetric stretch (3597 cm^{-1}), hydroxy O–H stretch (3749 cm^{-1}), azide N–N stretch (2283 cm^{-1}), nitro N–O asymmetric stretch (1649 cm^{-1}), ethynyl C–C asymmetric stretch (2227 cm^{-1}), ethenyl C–C asymmetric stretch (1689 cm^{-1}) and cyano C–N asymmetric stretch (2353 cm^{-1}) are, respectively, 177, 146, 576, 317, 127, 66 and 31 km mol^{-1}.

3.3 Potential candidates for high energy density materials

Nitrogen-rich compounds have attracted interest as well on account of their possible use as high energy density materials (HEDMs).[41–44] Bartlett[41] suggested some nitrogen-rich clusters formed by N, O, and H as HEDMs. Hammerl and Klapötke studied the nitrogen-rich clusters CN_x both experimentally and theoretically.[42] Nitrogen-rich compounds form a unique class of energetic materials, deriving most of their energy from their very high positive heats of formation rather than from oxidation of the carbon backbone, as with traditional energetic materials.[45] Usually, high heats of formation would decrease the stability of a compound. So the difficulty in identifying nitrogen-rich HEDM candidates lies in finding molecules that not only have high heats of formation but also are stable. All the compounds discussed in this paper have a extensive conjugation system, which would increase molecular stability. If their heats of formation are high enough, they may form a novel class of nitrogen-rich HEDMs.

The heat of formation, which is frequently taken to be indicative of the "energy content" of a HEDM, was calculated for tri-s-triazine and its derivatives. Moreover, as mentioned earlier, the specific impulse was also calculated to evaluate the performance of all these compounds as HEDMs. To facilitate comparisons, our values are given relative to HMX (1,3,5,7-tetranitro-1,3,5,7-tetraazacyclooctane), a widely used HEDM. In Table 7 are given idealized stoichiometric decomposition reactions for HMX, tri-s-triazine and its ten derivatives. According to Politzer *et al.*,[26] all nitrogens are assumed to go to N_2, carbons to C or CO (if oxygens are available), fluorines, chlorines, and bromines to F_2, Cl_2 and Br_2, while oxygens preferentially form H_2O (if hydrogens are available) or

Table 6 Selected harmonic vibrational frequencies and infrared (IR) intensities of tri-s-triazine (**A**) and its ten derivatives (**B1**–**B10**)

Molecule	Vibrational mode	Calculated		Exptal.
		Frequency/cm^{-1}	IR intensity/km mol^{-1}	Frequency/cm^{-1}
2,4,6-Triamino-s-triazine	Ring out-of-plane rocking	828	35	813
	Amino asymmetry stretch	3616	121	3500
2,4,6-Trifluoro-s-triazine,	Ring out-of-plane rocking	828	42	806
	C–F stretching	1087	130	1070
2,4,6-Trihydroxyl-s-triazine	Ring out-of-plane rocking	836	57	807
	Hydroxy asymmetry stretch	3759	157	3500
A	Ring out-of-plane rocking	870	35	
	C–H asymmetry stretch	3179	20	
B1	Ring out-of-plane rocking	856	41	
	Amino symmetry stretch	3597	177	
B2	Ring out-of-plane rocking	861	42	
	Hydroxy O–H stretch	3749	146	
B3	Ring out-of-plane rocking	861	37	
	Azide group N–N stretch	2283	576	
B4	Ring out-of-plane rocking	866	33	
	Nitryl N–O asymmetry stretch	1649	317	
B5	Ring out-of-plane rocking	867	36	
	Cyano C–N stretch	2353	31	
B6	Ring out-of-plane rocking	864	38	
B7	Ring out-of-plane rocking	864	34	
B8	Ring out-of-plane rocking	864	33	
B9	Ring out-of-plane rocking	870	40	
	Ethenyl C–C stretch	1689	66	
B10	Ring out-of-plane rocking	866	37	
	Ethynyl C–C stretch	2227	127	

Table 7 Idealized stoichiometric decomposition reactions and some properties of HMX, tri-s-triazine (**A**) and its ten derivatives (**B1**–**B10**)

Molecule	Reaction	n/M/mol.g^{-1}	$(n/M)^{\frac{1}{2}}$/mol.g$^{-\frac{1}{2}}$	Relative $\Delta_f H$	Relative I_s
HMX	$C_4N_8O_8H_8 \rightarrow 4CO + 4N_2 + 4H_2O$	0.0405	0.2013	1	1
A	$C_6N_7H_3 \rightarrow 7/2N_2 + 3/2H_2 + 6C$	0.0289	0.1700	1.34	0.73
B1	$C_6N_8H_4 \rightarrow 4N_2 + 2H_2 + 6C$	0.0319	0.1786	1.36	0.82
B2	$C_6N_7OH_3 \rightarrow 7/2N_2 + CO + 3/2H_2 + 5C$	0.0317	0.1782	1.09	0.80
B3	$C_6N_{10}H_2 \rightarrow 5N_2 + H_2 + 6C$	0.0280	0.1674	2.04	0.93
B4	$C_6N_8O_2H_2 \rightarrow 4N_2 + CO + H_2O + 5C$	0.0275	0.1659	1.55	0.94
B5	$C_7N_8H_2 \rightarrow 4N_2 + H_2 + 7C$	0.0252	0.1589	1.66	0.88
B6	$C_6N_7FH_2 \rightarrow 7/2N_2 + HF + 1/2H_2 + 6C$	0.0262	0.1618	1.15	0.60
B7	$C_6N_7ClH_2 \rightarrow 7/2N_2 + HCl + 1/2H_2 + 6C$	0.0242	0.1554	1.35	0.82
B8	$C_6N_7BrH_2 \rightarrow 7/2N_2 + HBr + 1/2H_2 + 6C$	0.0198	0.1409	1.42	0.74
B9	$C_8N_7H_5 \rightarrow 7/2N_2 + 5/2H_2 + 8C$	0.0301	0.1736	1.48	0.83
B10	$C_8N_7H_3 \rightarrow 7/2N_2 + 3/2H_2 + 8C$	0.0254	0.1593	1.79	0.91

otherwise CO and CO_2 in that order. We used such reactions to calculate the quantity n/M in which n is the number of moles of gaseous products and M is the molecular weight of the compounds. n/M provides a rough (and quickly determined) estimate of the number of moles of gaseous products available per unit weight of compound. Also included in Table 7 are the relative heats of formation obtained from calculated values (however, in computing the combustion temperature, the actual heats of formation were used).

Our calculated results point out quite clearly that **B3** with an azide group, **B4** with a nitro group and **B10** with an ethynyl group are potential candidates for HEDMs. Their specific impulses I_s (relative to HMX) are 0.93 for **B3**, 0.94 for **B4**, and 0.91 for **B10**. The introduction of azide, nitro and ethynyl groups increases the specific impulse compared to other substituents, which can be attributed to the greater heats of formation of these compounds. The relative heats of formation are 2.04 for **B3**, 1.55 for **B4** and 1.79 for **B10** compared to HMX. But all these three compounds have fairly low n/M values (0.0280 mol.g^{-1} for **B3**, 0.0275 mol.g^{-1} for **B4** and 0.0254 mol.g^{-1} for **B10**).

4. Summary

In this paper, we have investigated the geometries, electronic structures, harmonic vibrational frequencies and high energy density material properties of tri-s-triazine and ten of its derivatives. Tri-s-triazine has a rigid plane geometry with D_{3h} symmetry and shows considerable conjugation over the heterocycle, which is advantageous for its stability. From vibrational analysis, the ring has a characteristic frequency at 870 cm^{-1}, which could be used to distinguish tri-s-triazine from s-triazine. The electronic distribution in tri-s-triazine is very similar to that in s-triazine. When an electron-donating group or a substituent containing a π bond is attached to the parent ring, the lengths of the C–N bonds adjacent to the substituents increase, while when an electron-withdrawing group or a halogen is attached, these bond lengths decrease. However, in all these cases, the parent ring maintains its rigid plane. An MEP study shows that introduction of electron-donating groups and substituents containing a π bond (except –C≡N) on the parent ring will extend the negative spatial domains mildly, whereas introduction of halogens will shrink the negative spatial domains. A special case is when NO_2 and –C≡N groups are attached to the ring, causing the negative spatial domains to split and shrink, and new negative spatial domains to emerge near the nitryl oxygen and cyanophoric nitrogen. For all derivatives, calculated results indicate that the large conjugation system still exists and the characteristic frequency of the parent ring is around 850–870 cm^{-1}, shifted to higher wave number compared with that in tri-s-triazine. A molecular orbital study shows that the LUMO of all the derivatives is shared over all the atoms while the HOMO is localized on the peripheral nitrogen atoms of the ring. All the HOMO and LUMO are composed of $2p_z$ atomic orbitals. The introduction of a group containing a π bond on the parent ring will result in a decrease of the HOMO-LUMO energy gap. Moreover, our study shows that some of our discussed compounds may be potential candidates for high energy density materials (HEDMs), in particular those containing azide, nitro and ethynyl groups.

Acknowledgements

This work was supported by the Research Grants Council of Hong Kong (Project No. 9040742 CityU 1114/02P), Special Research Foundation of Doctoral Education of Chinese University (20020610024) and the National Science Foundation of China (298730029).

References

1 Z. Zhan, M. Müllner and J. A. Lercher, *Catal. Today*, 1996, **27**, 167.
2 (*a*) A. I. Finkel'shtein, *Opt. Spektrosk.*, 1959, **6**, 33; (*b*) K. Morokuma, T. Yonezawa and K. Fukui, *Bull. Chem. Soc. Jpn.*, 1962, **35**, 1646; (*c*) H. Saigusa and E. C. Lim, *J. Chem. Phys.*, 1983, **78**, 91; (*d*) S. R. Goates, J. O. Chu and G. W. Flynn, *J. Chem. Phys.*, 1984, **81**, 4521; (*e*) M. Zaruba, D. Hilt and G. S. Tennekoon, *Biochem. Biophys. Res. Commun.*, 1985, **129**, 522; (*f*) A. A. Korkin and R. J. Bartlett, *J. Am. Chem. Soc.*, 1996, **118**, 12 244; (*g*) T. W. Stringfield and R. E. Shepherd, *Inorg. Chim. Acta*, 1999, **292**, 225.
3 A. A. Korkin and R. J. Bartlett, *J. Am. Chem. Soc.*, 1996, **118**, 12 244.
4 J. Liebig, *Ann. Pharm.*, 1834, **10**, 10.
5 L. Gmelin, *Ann. Pharm.*, 1835, **15**, 252.
6 L. Pauling and J. H. Sturdivant, *Proc. Natl. Acad. Sci. U.S.A.*, 1937, **23**, 615.
7 *Chem. Eng. News*, Aug. 7th, 2000, p. 62 and Oct. 2nd, 2000, pp. 8–9.
8 M. A. Rossman, N. J. Leonard, S. Urano and P. R. LeBreton, *J. Am. Chem. Soc.*, 1985, **107**, 3884.
9 R. S. Hosmane, M. A. Rossman and N. J. Leonard, *J. Am. Chem. Soc.*, 1982, **104**, 5497.
10 M. Shahbaz, S. Urano, P. R. LeBreton, M. A. Rossman, R. S. Hosmane and N. J. Leonard, *J. Am. Chem. Soc.*, 1984, **106**, 2805.
11 M. A. Rossman, R. S. Hosmane and N. J. Leonard, *J. Phys. Chem.*, 1984, **88**, 4324.
12 E. Kroke, M. Schwarz, E. H. Bordon, P. Kroll, B. Noll and A. D. Norman, *New J. Chem.*, 2002, **26**, 508.
13 (*a*) C. E. Redemann and H. J. Lucas, *J. Am. Chem. Soc.*, 1940, **62**, 842; (*b*) H. Schroeder and E. Kober, *J. Org. Chem.*, 1962, **27**, 4262; (*c*) H. Schroeder, *US Pat.*, 1963, US3089875 (Olin Mathieson Chem. Corp.); (*d*) A. I. Finkelshtein and N. V. Spiridonova, *Russ. Chem. Rev.*, 1964, **33**, 400; (*e*) R. Neef, *Ger. Pat.*, 1961 DE1102321 (Bayer AG); (*f*) C. Gremmelmaier and J. Riethmann, *US Pat.*, 1980, US 4205167A (Ciba-Geigy).

14 W. X. Zheng, N. B. Wong, W. Z. Wang, G. Zhou and A. M. Tian, *J. Phys. Chem. A*, 2004, **108**, 97.
15 R. G. Parr and W. Yang, *Density-Functional Theory of Atoms and Molecules*, Oxford University Press, New York, 1989.
16 A. D. Becke, *J. Chem. Phys.*, 1993, **98**, 5648.
17 C. Lee, W. Yang and R. G. Parr, *Phys. Rev. B*, 1988, **37**, 785.
18 D. E. Woon and T. H. Dunning, *J. Chem. Phys.*, 1993, **98**, 1358.
19 J. E. Carpenter and F. Weinhold, *J. Mol. Struct. (Theochem)*, 1988, **169**, 41.
20 A. E. Reed, L. A. Curtiss and F. Weinhold, *Chem. Rev.*, 1988, **88**, 899.
21 J. P. Foster and F. Weinhold, *J. Am. Chem. Soc.*, 1980, **102**, 7211.
22 A. E. Reed, R. B. Weinstock and F. J. Weinhold, *Chem. Phys.*, 1985, **83**, 735.
23 M. J. Frisch, G. W. Trucks, H. B. Schlegel, G. E. Scuseria, M. A. Robb, J. R. Cheeseman, V. G. Zakrzewski, J. A. Montgomery, Jr., R. E. Stratmann, J. C. Burant, S. Dapprich, J. M. Millam, A. D. Daniels, K. N. Kudin, M. C. Strain, O. Farkas, J. Tomasi, V. Barone, M. Cossi, R. Cammi, B. Mennucci, C. Pomelli, C. Adamo, S. Clifford, J. Ochterski, G. A. Petersson, P. Y. Ayala, Q. Cui, K. Morokuma, P. Salvador, J. J. Dannenberg, D. K. Malick, A. D. Rabuck, K. Raghavachari, J. B. Foresman, J. Cioslowski, J. V. Ortiz, A. G. Baboul, B. B. Stefanov, G. Liu, A. Liashenko, P. Piskorz, I. Komaromi, R. Gomperts, R. L. Martin, D. J. Fox, T. Keith, M. A. Al-Laham, C. Y. Peng, A. Nanayakkara, M. Challacombe, P. M. W. Gill, B. G. Johnson, W. Chen, M. W. Wong, J. L. Andres, C. Gonzalez, M. Head-Gordon, E. S. Replogle and J. A. Pople, *GAUSSIAN 98 (Revision A.11)*, Gaussian, Inc., Pittsburgh, PA, 2001.
24 R. F. W. Bader, *Atoms in Molecules, A Quantum Theory*, International Series of Monographs in Chemistry, Oxford University Press, Oxford, 1990, vol. 22.
25 F. Biegler-König, J. Schönbohm, R. Derdau, D. Bayles and R. F. W. Bader, *AIM 2000*, version 2.0, McMaster University, Hamilton, Canada, 2002.
26 P. Politzer, J. S. Murray, M. E. Grice and P. Sjoberg, in *Chemistry of Energetic Materials*, eds. G. A. Olah and D. R. Squire, Academic Press, San Diego, CA, 1991, pp. 77–93.
27 R. Mayer, *Explosives*, VCH, Weinheim, Germany, 1987.
28 J. E. Lancaster and B. P. Stoicheff, *Can. J. Phys.*, 1956, **34**, 1016.
29 A. F. Wells, *Structural Inorganic Chemistry*, 3rd edn., Oxford University Press, Oxford, 1962.
30 R. F. W. Bader and H. Essen, *J. Chem. Phys.*, 1984, **80**, 1943.
31 R. F. W. Bader, P. J. MacDougall and C. D. H. Lau, *J. Am. Chem. Soc.*, 1984, **106**, 1594.
32 P. Politzer and J. S. Murray, in *Molecular Electrostatic Potentials: Concepts and Applications*, eds. J. S. Murray and K. D. Sen, Elsevier, Amsterdam, 1996, p. 649.
33 B. Boris and B. Petia, *J. Phys. Chem. A*, 1999, **103**, 6793.
34 S. R. Gadre and P. K. Bhadane, *J. Phys. Chem. A*, 1999, **103**, 3512.
35 J. S. Murray and P. Politzer, in *Encyclopedia of Computational Chemistry*, ed. P. R. Schleyer, Wiley, New York, 1998, vol. 2, p. 912.
36 C. J. Cramer, *Essentials of Computational Chemistry: Theories and Models*, Wiley, Chichester, UK, 2002, p. 278.
37 K. Fukui, *Theory of Orientation and Stereoselection, Reactivity and Structure, Concepts in Organic Chemistry*, Springer, Berlin, 1975, vol. 2.
38 U. Salzner, *Synth. Met.*, 1999, **101**, 482.
39 A. Szabo and N. S. Ostlund, *Modern Quantum Chemistry: Introduction to Advanced Electronic Structure Theory*, McGraw-Hill, New York, 1982.
40 *The Aldrich Library of Infrared Spectra*, ed. C. J. Pouchert, Aldrich Chemical Company, Milwaukee, WI, 1981.
41 R. Bartlett, *Chem. Ind.*, 2000, **21**, 140.
42 A. Hammerl and T. M. Klapötke, *Inorg. Chem.*, 2002, **41**, 906.
43 L. Gagliardi and P. J. Pyykkö, *J. Am. Chem. Soc.*, 2001, **123**, 9700.
44 L. Gagliardi and P. J. Pyykkö, *J. Phys. Chem. A*, 2002, **106**, 4690.
45 (*a*) M. X. Zhang, P. E. Eaton and R. D. Gilardi, *Angew. Chem.*, 2000, **112**, 422; (*b*) M. X. Zhang, P. E. Eaton and R. D. Gilardi, *Angew. Chem., Int. Ed.*, 2000, **39**, 401.